THE JOURNAL OF PHYSICAL CHEMISTRY C

Article

pubs.acs.org/JPCC

Photoelectron Spectroscopy Study of Stoichiometric and Reduced Anatase TiO_2(101) Surfaces: The Effect of Subsurface Defects on Water Adsorption at Near-Ambient Pressures

Mark J. Jackman,[†,‡] Andrew G. Thomas,*[,‡] and Chris Muryn[§]

[†]School of Physics and Astronomy and Photon Science Institute, [‡]School of Materials and Photon Science Institute, and [§]Chemistry and Photon Science Institute, Alan Turing Building, The University of Manchester, Oxford Road, Manchester M13 9PL, United Kingdom

Supporting Information

ABSTRACT: X-ray photoelectron (XPS) experiments at normal and grazing emission are performed, demonstrating the labile nature of the anatase TiO_2(101) surface after argon cluster ion sputtering and the propensity of oxygen vacancies to migrate subsurface at room temperature. Near-ambient XPS (NAP-XPS) shows that molecular water adsorbs on the anatase TiO_2(101) surface at pressures of 0.6 mbar and above, at room temperature, in a mixed molecular and dissociated state. Water adsorbs in a similar fashion on both sputtered and stoichiometric surfaces and reaches a saturation point between 0.6 and 1.8 mbar at room temperature. This means there is little difference in reactivity with regards to water adsorption on both sputtered and stoichiometric surfaces, giving credence to the theory that anatase has superior photocatalytic activity over rutile due to the tendency of oxygen vacancies to lie subsurface, therefore being able to contribute to photocatalysis without being quenched by adsorbates.

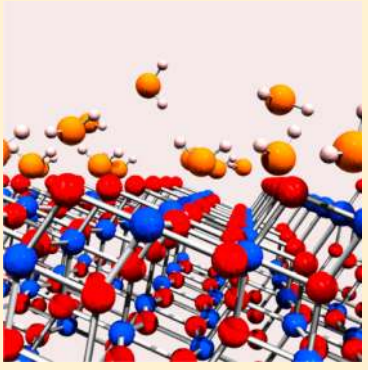

INTRODUCTION

The two most studied faces of TiO_2 are the rutile (110) and the anatase (101) surfaces. Rutile is the most thermodynamically stable surface at higher temperatures, whereas anatase, a natural-forming polymorph, is the most stable at room temperature.[1] The optical bandgap of TiO_2 at low temperatures is 3.420 eV for anatase and 3.035 eV for rutile,[2] meaning titania absorbs the ultraviolet part of the solar spectrum. Efforts have been made to alter the bandgap with doping,[3] nanocrystalline structures,[4] and dyeing;[5] the latter has been successful for dye-sensitized solar cells.[6] Anatase is also the most photoactive of the polymorphs, although mixed anatase/rutile powders are more photoactive still.[7,8] This is thought to occur due to the relative band positions of the two polymorphs whereby photoexcited electrons in rutile flow from its conduction band into that of the anatase.[8] P25, a standard industrial nanoparticulate TiO_2 photocatalyst, is a mix of anatase and rutile.

The interaction with water and TiO_2 underpins many processes that drive commercial applications including self-cleaning surfaces,[9] dye-sensitized solar cells,[10,11] and solar water-splitting.[12] Figure 1 shows the (101) surface of anatase TiO_2. Single-crystal anatase is an n-type semiconductor when doped through the formation of bulk oxygen vacancies, which are created when preparing crystal surfaces by sputter and anneal cycles.[1] Reduction of the TiO_2 surface results in the appearance of a feature at a binding energy of 1 eV in the valence band photoemission spectrum. Resonant photoemission has confirmed the Ti 3d nature of this state in both anatase and rutile single crystals.[13] This feature also has also been shown to contain contributions from step edges,[14] and it has been suggested that titanium interstitials also contribute to its intensity.[15]

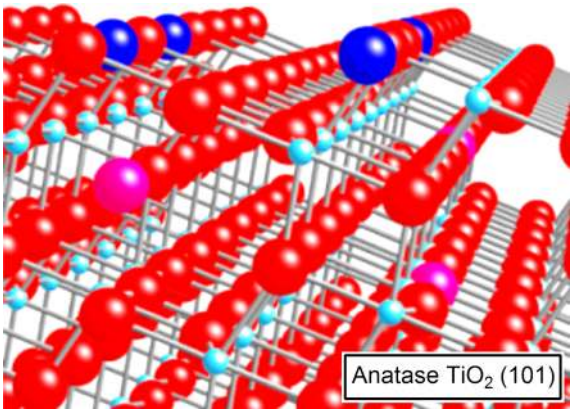

Figure 1. Anatase (101) surface. Red atoms are oxygen; light blue are titanium. Dark blue atoms represent surface oxygen vacancies, and the pink atoms represent subsurface oxygen vacancies.

It has long been postulated that defects at the surface in the form of O-vacancies or step edges are catalytic centers in TiO_2. The reason for the superior photocatalytic activity of anatase

Received: March 20, 2015
Revised: May 18, 2015
Published: May 25, 2015

DOI: 10.1021/acs.jpcc.5b02732
J. Phys. Chem. C 2015, 119, 13682−13690

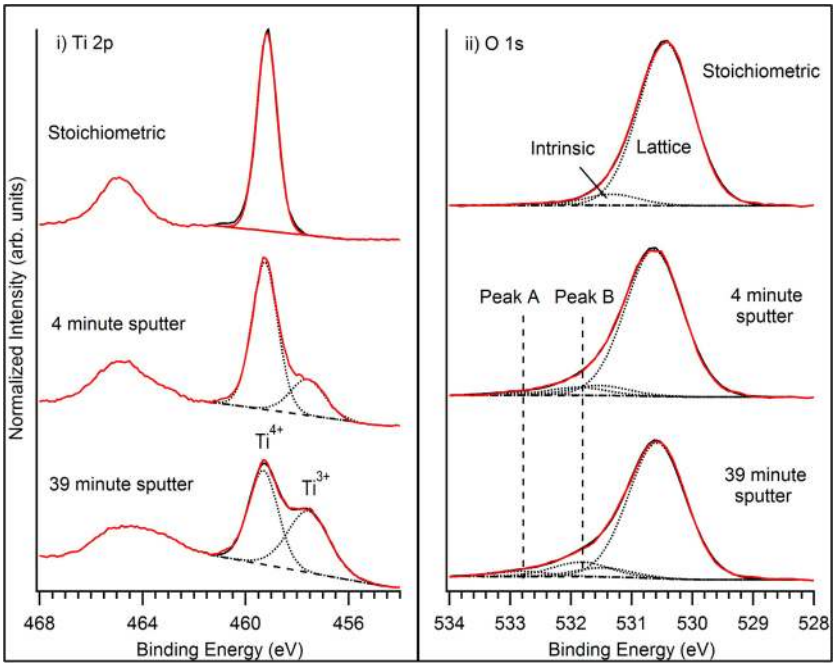

Figure 2. Peak fitting for defect creation with the argon cluster ion source for the Ti 2p and O 1s spectra.

over rutile has been attributed to the defects at the anatase $TiO_2(101)$ surface tending to lie subsurface[16,17] (see Figure 1). Defect sites trap photoexcited charge carriers, and if oxygen vacancies are present on the surface, as in rutile $TiO_2(110)$, they will be quenched by adsorption of ambient molecules. However, if they sit just below the surface as in anatase $TiO_2(101)$, they avoid quenching and contribute to photocatalysis. The nature of these defects continues to inspire debate both experimentally[14,18] and theoretically.[19] It is the location of these defects, surface vs subsurface, and the interaction with water which form the basis of the work presented here.

Until recently, understanding the fundamental electronic and chemical environment of surfaces utilizing X-ray photoelectron spectroscopy (XPS) has required analysis in high vacuum, but advances in electron optics have led to the development of XPS at near-ambient pressures. There is a wealth of information available regarding the interaction of TiO_2 and water exposure at low pressure as the surfaces have been studied intensively. Walle et al. investigated the mixed dissociative adsorption of water on anatase $TiO_2(101)$ at temperatures from 160 to 400 K[20] and showed that water dosed on the surface at room temperature dissociates to form hydroxylated anatase. This contradicts previous work including that carried out using STM[21] and XPS[22] but is supported by first-principles calculations.[23] Near-ambient XPS is still a relatively new technique, but water adsorption has been studied on MgO films[24] and GaAs(100).[25] Unsurprisingly, TiO_2 has been studied in near-ambient systems. Haubrich et al. investigated the interaction with water and NO_2 on rutile $TiO_2(110)$,[26] whereas Destaillats et al. investigated similar molecules on anatase, as well as the effects of UV irradiation.[27] Closely related to the work carried out here is that by Ketteler et al.[28] who studied the effects of water nucleation on sputtered rutile (110).

Here we study the nature of the defects created by an argon ion cluster sputter source on single-crystal anatase $TiO_2(101)$ using a monochromated Al K-α X-ray at high vacuum (3×10^{-9} mbar). Comparisons between the Ti 2p spectra are made with the O 1s spectra at normal and grazing emission, and we show that oxygen vacancies created at the surface migrate to the subsurface. We then investigate the exposure of the stoichiometric and sputtered anatase $TiO_2(101)$ surfaces to water at pressures of 0.6, 1.8, and 6.0 mbar and show that water adsorbs in a similar fashion on both surfaces, both dissociative and molecular. Water adsorption reaches a saturation point between 0.6 and 1.8 mbar on both surfaces at room temperature.

EXPERIMENTAL SECTION

The near-ambient pressure (NAP) XPS system employed in this work is equipped with a SPECS Focus 500 monochromated Al Kα source (photon energy 1486.6 eV), which can be focused to a spot size of 300 μm. The analyzer is a SPECS 150 mm Phoibos 150 NAP, fitted with a three-stage, differentially pumped electrostatic lens that allows working pressures up to 25 mbar and a 44° acceptance angle. NAP-XPS measurements are made in a specially designed cell which couples to the entrance cone of the analyzer lens system.

The anatase $TiO_2(101)$ single crystal (5 mm^2, Pi-kem Ltd.) was cut from a natural crystal. The crystals were held in place on stainless steel sample plates by four strips of tantalum wire. The crystal was cleaned by repeated Ar_{800}^+ cluster ion etching at a cluster energy of 10 keV and annealing to 650 °C (measured by a pyrometer) in vacuum. This treatment is well established in producing a stoichiometric anatase $TiO_2(101)$ surface with a 1 × 1 termination free from contamination by carbon.[13,14,29] See Supporting Information S.1 for the wide scan.

Doubly distilled water was degassed by several freeze−pump−thaw cycles and was dosed from a glass tube, heated to 60 °C. The clean anatase $TiO_2(101)$ surface was analyzed at 3×10^{-9} mbar and under exposure to water pressures of 0.6, 1.8, and 6 mbar in the high-pressure cell. The high-pressure cell was then evacuated and the sample analyzed again once a pressure

DOI: 10.1021/acs.jpcc.5b02732
J. Phys. Chem. C 2015, 119, 13682−13690

Table 1. Component Analysis of the Defect Formation with Argon Cluster Sputtering[a]

	Component	Sputter time (mins) 0	2	4	14	24	39
% of Ti $2p_{3/2}$	Ti^{4+} 459.2 eV	100.0	82.9	75.7	62.7	58.0	52.3
	Ti^{3+} 457.5 eV	0.0	17.2	24.3	37.3	42.0	47.7
% of O 1s	O lattice 530.5 eV	92.7	87.3	87.4	84.4	82.7	82.4
	$O_{intrinsic}$ 531.6 eV	6.3	6.0	6.0	5.7	5.6	5.6
	Peak A 531.8 eV	-	4.4	4.9	7.4	8.4	8.9
	Peak B 532.8 eV	1.0	2.3	1.7	2.5	3.2	3.1
Ti $2p_{3/2}$	FWHM Ti^{4+}	0.88	1.11	1.18	1.27	1.28	1.33
	FWHM Ti^{3+}	-	1.48	1.57	1.66	1.77	1.88
O 1s	FWHM	1.05	1.10	1.11	1.10	1.11	1.11

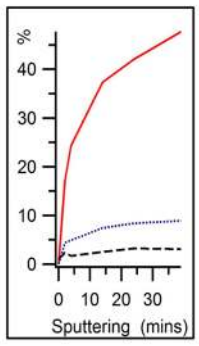

[a]The inset graph shows the intensity of peak A (blue-dotted) and B (black-dashed) in the O 1s spectra and Ti^{3+} (red-solid) in the Ti $2p_{3/2}$ spectra as a function of sputtering time.

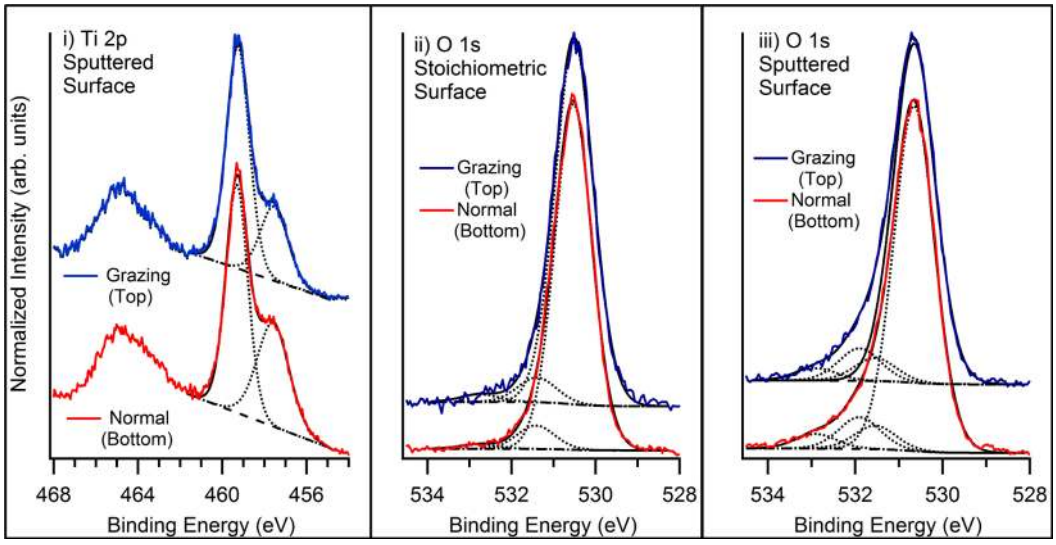

Figure 3. Ti 2p and O 1s spectra of sputtered and stoichiometric surface at normal (red, bottom spectra) emission and at 60° grazing angle (blue, top spectra).

of 1×10^{-8} mbar had been obtained. Water adsorption was investigated on the annealed, stoichiometric surface and a reduced surface that was created by sputtering the surface using the cluster ion source (Ar_{800}^{+}, 10 keV cluster energy) for 2 min before analysis. All spectra are aligned on the binding energy (BE) scale with reference to the Fermi level, and BE values are quoted to ±0.1 eV. A Shirley background was subtracted from the data, and 70% Gaussian:30% Lorentzian curves were used to fit the core-level spectra using CASA XPS (CASA Software Ltd.).

RESULTS AND DISCUSSION

I. Clean Stoichiometric and Ar^{+} Ion Bombarded Anatase TiO_2(101) Surfaces. Figure 2 shows XPS spectra following defect creation with the argon cluster ion source as a function of time for the Ti 2p and the O 1s spectra. Table 1 details the component analysis obtained from these spectra. Spectra were taken at 2, 4, 14, 24, and 39 min, and the surface was analyzed immediately after sputtering. The doublet in the Ti 2p spectra arises from spin orbit-splitting Ti $2p_{3/2}$ and Ti $2p_{1/2}$.[30] For simplicity, peak fitting is only carried out on Ti $2p_{3/2}$, which for the annealed stoichiometric anatase TiO_2(101) surface has a binding energy of 459.2 eV. On sputtering, a shoulder due to the creation of Ti^{3+} at 457.5 eV BE[31,32] is observed as oxygen is removed from the surface resulting in two Ti^{3+} atoms.[1] As can be seen from Table 1, the fwhm of the Ti 2p components increases with sputtering. This is partly due to the different shapes of TiO_2 and Ti_2O_3 spectra.[33] It is possible that some Ti^{2+} is formed when the surface is heavily reduced. Ti^{2+} is observed at energies of approximately 456 eV;[34] however, a good fit is obtained without adding this extra component.

We turn now to the O 1s spectrum where the main peak at 530.5 eV is attributed to lattice oxygen.[35] In order to obtain a satisfactory fit, a second component must also be fitted at a slightly higher binding energy of 531.4 eV. The intensity of this peak does not change between normal and grazing emission angles as shown in Figure 3. It has been suggested that this peak could be surface related, arising from bridging oxygens in the case of rutile TiO_2(110)[36] or from adsorbed hydroxide,[20]

DOI: 10.1021/acs.jpcc.5b02732
J. Phys. Chem. C 2015, 119, 13682−13690

Table 2. Component Analysis for Ti 2p and O 1s Spectra of Sputtered and Stoichiometric Surface at Normal (N) and at 60° Grazing (G) Emission Angles

	Ti $2p_{3/2}$ %		O 1s %			
surface	Ti^{4+} 459.2 eV	Ti^{3+} 457.5 eV	lattice 530.5 eV	intrinsic 531.4 eV	peak A 531.8 eV	peak B 532.8 eV
sputtered N	59.4	40.6	84.1	5.7	7.4	2.8
sputtered G	71.8	28.2	83.7	5.7	7.9	2.7
stoichiometric N	–	–	92.4	6.3	–	1.3
stoichiometric G	–	–	91.8	6.3	–	2.0

but in both of these cases one would expect to observe an increase in intensity with respect to the main oxide peak upon moving to a grazing emission angle where the surface sensitivity is higher. Thus, the data here suggest that this feature arises from a species intrinsic to the lattice, i.e., a species or chemical environment which is found both at the surface and the bulk/selvedge at similar concentrations, or that the O 1s peak contains some natural asymmetry. Hard-X-ray photoelectron spectroscopy, which allows the bulk chemistry and electronic structure of a material to be probed,[37] suggests this higher binding energy peak is an intrinsic feature of the O 1s spectrum, either a separate component or arising from an asymmetric peak shape (see Supporting Information S.2). To account for this, all O 1s spectra are fitted with a component ($O_{intrinsic}$) at a binding energy and intensity fixed relative to the main oxide peak as derived from the spectrum recorded from the stoichiometric surface.

We also note that component analysis of the O 1s is complicated due to a broad energy loss feature centered ~6.2 eV to higher binding energy relative to the O 1s spectrum, associated with excitation across the band gap[38] which causes difficulty with the background fitting, potentially leading to the appearance of artifacts. A small peak observed in the grazing emission spectrum at 532.8 eV BE, for example, may arise from some oxygen-containing hydrocarbon contamination[27] but could also be an artifact of the background fitting.

Sputtering the anatase $TiO_2(101)$ surface results in two features (labeled A and B) appearing in the O 1s spectra to the higher binding energy side of the lattice oxygen, which increase in size with sputtering time. This has also been observed on the rutile $TiO_2(110)$ surface where the O 1s spectrum was monitored through defect creation with ion bombardment and thermal treatment.[39] The shift to higher binding energy species is attributed to electron transfer from oxygen to titanium.[39] However, it is difficult to rule out the adsorption of oxygen-containing organic species or water/hydroxide since these give rise to features in the O 1s spectrum at similar energies to those seen following etching. Spectra were obtained directly after sputtering, and no C 1s peaks were present in XPS spectra; however, carbon-containing species could appear over the course of the analysis since the pressure in the main chamber was 3×10^{-9} mbar. Surface hydroxyls appear at a similar binding energy. On the anatase $TiO_2(001)$ surface, adsorption of up to 2.5 L of water at 190 K followed by heating of the film leads to the appearance of peaks at +1.55 and +3.55 eV relative to the lattice oxygen.[40] These peaks were assigned to hydroxyls and water, respectively.[40] On the anatase $TiO_2(101)$ surface, below 250 K, the O 1s photoemission peak of water appears 3.5 eV higher than lattice oxygen.[41] On the rutile $TiO_2(110)$ surface, the water O 1s peak appears at 2.4−3.4 eV higher and the hydroxyl peak at 1.1−1.6 eV higher[28] in relation to the substrate O 1s peak.

It is not possible to fit a single peak to the feature or features that grow with argon cluster sputtering without fitting an extremely broad peak with a fwhm twice that of the lattice oxygen-derived peak (a method that was employed by Walle et al. in their study on water adsorption[20]). Therefore, two peaks have been fitted at 531.8 and 532.8 eV BE to account for changes in the O 1s spectrum associated with the growth of defects. Note that the peak at 531.8 eV is very close to the intrinsic feature at 531.6 eV and could be fitted as a single peak, but this would imply the intrinsic feature grows with sputtering which cannot be ascertained from our data. The plot in Table 1 shows how the intensities of the defect-induced peaks in the O 1s spectra change over time. It appears that the O 1s defect components are related as they increase at a similar rate. G. Lu et al. subjected polycrystalline titanium metal to an oxygen atmosphere and analyzed by XPS.[31] They observed an asymmetric O 1s peak consisting of two symmetrical peaks, one from TiO_2 at 530.1 eV and the other at 531.2 eV, which they believe is likely due to TiO.[31] However, the Ti 2p spectrum indicates there is no or little TiO formed in our system as only Ti^{3+} is observed. We also note that, unlike the Ti 2p spectrum, there is no change in the fwhm of the O 1s peak. The reasons for that are not clear but may be due to the fact that Ti 2p spectra of the sesquioxide Ti_2O_3 tend to exhibit broader peaks than TiO_2,[33,42] possibly due to final state effects involving the singly occupied d-orbital. In O 1s spectra, on the other hand, there is only a 0.1 eV shift between TiO_2 and Ti_2O_3 derived O 1s peaks,[43] which cannot be resolved; thus, the broadening is not seen.

The complexity of the component analysis is increased due to the migration of surface defects to the subsurface region, something that has been demonstrated by STM on an anatase $TiO_2(101)$ surface.[44]

Figure 3 shows the Ar cluster ion sputtered Ti 2p spectrum recorded at normal and grazing (60° from normal) emission angles, and O 1s spectra for the stoichiometric and sputtered surfaces at normal (NE) and grazing (GE) emission. One can clearly see from Table 2 that at a 60° emission angle the Ti 2p spectrum changes and the Ti^{3+} component is reduced. For Ti $2p_{3/2}$ electrons, using Al Kα X-rays the sampling depth is 9.2 nm at normal emission, and at 60° it is 4.6 nm.[45] This implies that the oxygen vacancies are moving below the surface, although we cannot say with any certainty how these oxygen vacancies are distributed through the subsurface. Based on the ratios of Ti^{3+}:Ti^{4+} at normal and grazing emission, there are approximately 1.4 times fewer oxygen vacancies in the top 5 nm of the surface than there are in the subsequent 5 nm of subsurface.

With regard to the O 1s spectra recorded at NE and GE, there is no significant difference between the intensities of peaks A and B; thus, the origin of peaks A and B is unclear. The increased asymmetry to the higher binding energy side of the O 1s peak is consistent with that reported for Ar^+ sputtered rutile

DOI: 10.1021/acs.jpcc.5b02732
J. Phys. Chem. C 2015, 119, 13682−13690

TiO_2(110) as mentioned above and suggests these vacancy sites are distributed through the surface and subsurface region. This, however, would appear to be at odds with the Ti 2p data, which suggest that Ti^{3+} is located predominantly subsurface as there are no changes in the intensities of peaks A and B with emission angle. Peak A is located 1.3 eV to higher BE relative to the main oxide O 1s peak. This energy is consistent with a loss feature observed in electron energy loss spectra of electron bombarded[46] and Ar^+ bombarded TiO_2 surfaces.[47] The loss feature is rather broad and may therefore account for both peaks A and B. The relative intensities of peaks A and B are consistent with a single and double energy loss process.[47] However, even in this case one would still expect a decrease in the intensity of peaks A and B relative to the main O 1s peak at grazing emission angles since the loss process is thought to involve Ti^{3+} species.[39,46,47]

II. Near-Ambient Pressure Water Exposure. Figure 4 shows the Ti 2p spectra for the stoichiometric and sputtered surface of anatase at high vacuum (3×10^{-9} mbar) and during exposure to water at pressures of 0.6, 1.8, and 6.0 mbar. We also show the spectrum obtained after pumping the analysis chamber back down to 1×10^{-8} mbar. The Ti 2p spectra recorded from the stoichiometric surface show no changes upon exposure to water even at the highest pressure of 6.0 mbar.

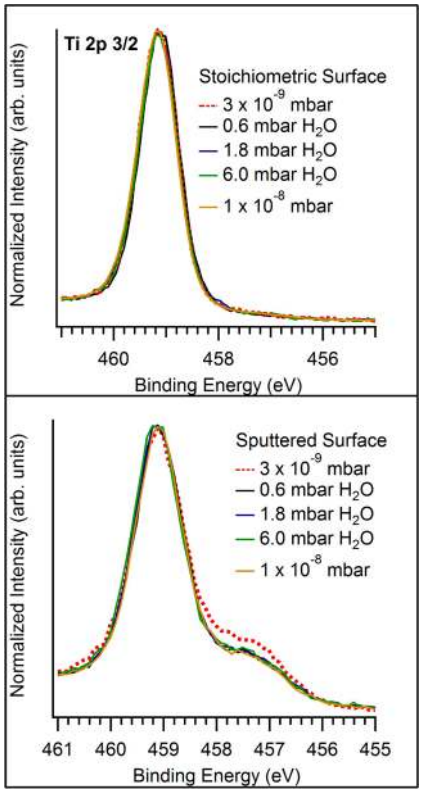

Figure 4. Ti $2p_{3/2}$ spectra of the sputtered and stoichiometric surfaces of anatase TiO_2(101) at increasing pressures. The orange spectra was taken at 1×10^{-8} mbar, after the water at 6 mbar has been pumped out of the high-pressure cell.

There is a clear reduction in the intensity of the Ti^{3+}-derived feature upon exposure to 0.6 mbar, but with increasing water pressure no further changes in the Ti 2p spectrum are observed. Ketteler et al. also observed a reduction in Ti^{3+} when dosing water at 0.1 mTorr on rutile.[28] A reduction in the Ti^{3+} can be interpreted in two ways: (i) defects have migrated from the surface over time, and (ii) the Ti^{3+} components have been oxidized to Ti^{4+} during adsorption of water. This phenomenon has been observed with the interaction of small molecules such as N_2O, O_2, H_2O, and HCOOH on the rutile surface.[48] Li and Gao performed first principles calculations, studying the effects of water and the anatase TiO_2(101) surface with both surface and subsurface vacancies.[49] They calculated the surface vacancy to be more stable than the subsurface vacancy when water is adsorbed on the surface. This is in contrast to DFT calculations by Deák et al. where it was shown that surface oxygen vacancies are more stable than subsurface oxygen vacancies without the presence of water.[50] It is clear from our results that there is no migration of vacancies to the surface.

Figure 5 shows the O 1s spectra for the sputtered and stoichiometric surfaces at high vacuum and during exposure to 0.6, 1.8, and 6.0 mbar H_2O. We also show the O 1s spectrum recorded following the water exposure experiments after the high-pressure cell had been evacuated and the pressure had returned to 1×10^{-8} mbar. A spectrum recorded from gas-phase water, where the sample was drawn away from the analyzer so only water vapor was in the X-ray beam, is shown by the blue line. For both the stoichiometric and sputtered surfaces, three additional components can be fitted to the O 1s peak at 531.7, 532.7, and 533.5 eV, in addition to the gas-phase water derived feature in the spectra recorded upon exposure to water vapor at 0.6, 1.8, and 6.0 mbar. Peak fitting to these spectra is difficult and in the case of the sputtered surface further complicated by the fact that if the two O 1s peaks (peak A and peak B in the discussion above) are associated with oxygen vacancies then one may expect them to be reduced in intensity upon exposure to water, as is the case for Ti^{3+}-related features in the Ti 2p spectra.

In an attempt to examine the effects of water adsorption, we have generated difference spectra as shown in Figure 6. Figures 6a and 6b are recorded from the stoichiometric and sputtered surfaces, respectively, and are obtained by subtracting the fitted Gaussian:Lorentzian (GL) peaks for the oxide and the "intrinsic" peaks. The peak at ~530.0 eV in both sets of spectra is an artifact of the subtraction procedure since the fitted GL peak does not fit perfectly on the low BE side of the O 1s oxide peak.

For the stoichiometric surface, this simply results in a spectrum showing the features due to the exposure to water. The broad peaks obtained by this subtraction process suggest multiple components. Lines have been drawn on the spectra at binding energies of 531.7 and 533.5 eV, which correspond to adsorbed hydroxide and molecular water on the rutile TiO_2 (110) surface, respectively.[27,51] The weighting of the peak suggests roughly equal amounts of molecularly adsorbed water and OH. For the sputtered surface, the picture is not so clear. At first glance it appears that the peak resulting from the subtraction process is more heavily weighted to OH. However, in only subtracting the fitted oxide and intrinsic peaks we have not accounted for the two peaks that appear as a result of sputtering the surface. It is not possible to subtract these peaks reliably as we are unable to determine whether peak A and peak B (as they were referred to above) change in intensity upon exposure to water. One possible clue to the nature of water adsorption at near-ambient pressures on the sputtered surface is shown by subtracting the oxide and "intrinsic" peak from the clean sputtered surface spectrum, as shown by the brown

DOI: 10.1021/acs.jpcc.5b02732
J. Phys. Chem. C 2015, 119, 13682−13690

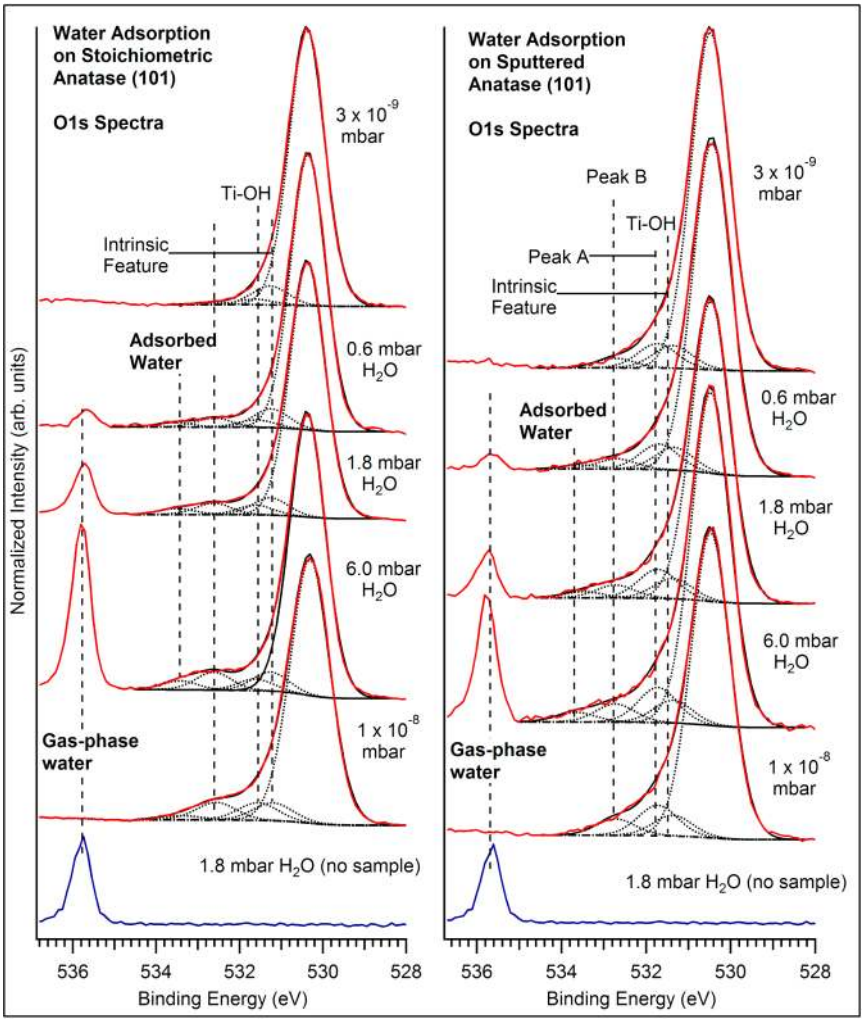

Figure 5. O 1s spectra of the sputtered and stoichiometric surfaces of anatase $TiO_2(101)$ at increasing pressures The spectra labeled 1×10^{-8} mbar are recorded after exposure to water at 6 mbar. The binding energy positions of some oxygen-containing species which may give rise to peaks in this region have also been shown, although as described in the text there is no evidence of oxygen-containing carbon species in the C 1s spectra.

dotted spectrum in Figure 6b. This spectrum is clearly weighted around the OH region, whereas the difference spectra have appreciable intensity in the molecular water region. This suggests that the sputtered surface also shows mixed molecular and dissociative water adsorption at near-ambient pressures. Figures 6c and 6d also show difference spectra for the stoichiometric and sputtered surfaces. These difference spectra are generated by normalizing to the height of the oxide peak at 530.5 eV in Figure 5, then subtracting the previous spectrum to show the effects of subsequent exposure (i.e., the clean surface is subtracted from the 0.6 mbar exposed surface, the 0.6 mbar from the 1.8 mbar, etc.). This shows that when increasing the pressure from 1.8 mbar to 6.0 mbar there is little change in the O 1s spectrum suggesting a saturation point for water adsorption on this surface at room temperature. To increase water adsorption, the temperature could be lowered or the pressure raised, thus increasing the relative humidity further, as observed on the rutile $TiO_2(110)$ surface.[52]

The O 1s spectra may be further complicated by the possible presence of oxygen-containing organic species. Carbon contamination is an inherent problem with high-pressure systems.[28] Oxygen-containing carbon compounds often make up background contamination, which is exacerbated at higher pressures as water dosed into the system displaces organics, CO, and CO_2 from the chamber walls. When characterizing NO_2/water adsorption on anatase $TiO_2(101)$, Rosseler et al. observed two peaks, one at 1.1−1.6 eV higher than the lattice oxygen that was assigned to hydroxyl groups at bridging sites and also C═O species.[27] Although we have identified molecular water and hydroxide in the difference spectra, in light of the issues with carbon contamination mentioned above there is also the possibility that there is some C═O component at this energy.[27] However, a C 1s spectrum obtained from the surface which had become contaminated after several hours in high vacuum showed no evidence of C═O or C−O side groups (see Supporting Information S.3). The origin of the C contamination in this work is unclear. Work on CO and CO_2 adsorption on stoichiometric and reduced rutile $TiO_2(110)$[53] and anatase powders[54] suggests the molecules do not adsorb above −73 °C in ultra-high vacuum (UHV); however, no work at high pressures of CO and CO_2 has been performed. In addition, a theoretical study of CO_2 adsorption on anatase suggested oxygen exchange occurs, whereby CO_2 exchanges oxygen with the surface before desorbing again as CO_2.[55]

The features at binding energies of 531.7, 532.7 eV in the O 1s spectra recorded after exposure to 6 mbar of which was then pumped away to restore a vacuum of 1×10^{-8} mbar remain visible for both the stoichiometric and sputtered surfaces

DOI: 10.1021/acs.jpcc.5b02732
J. Phys. Chem. C 2015, 119, 13682−13690

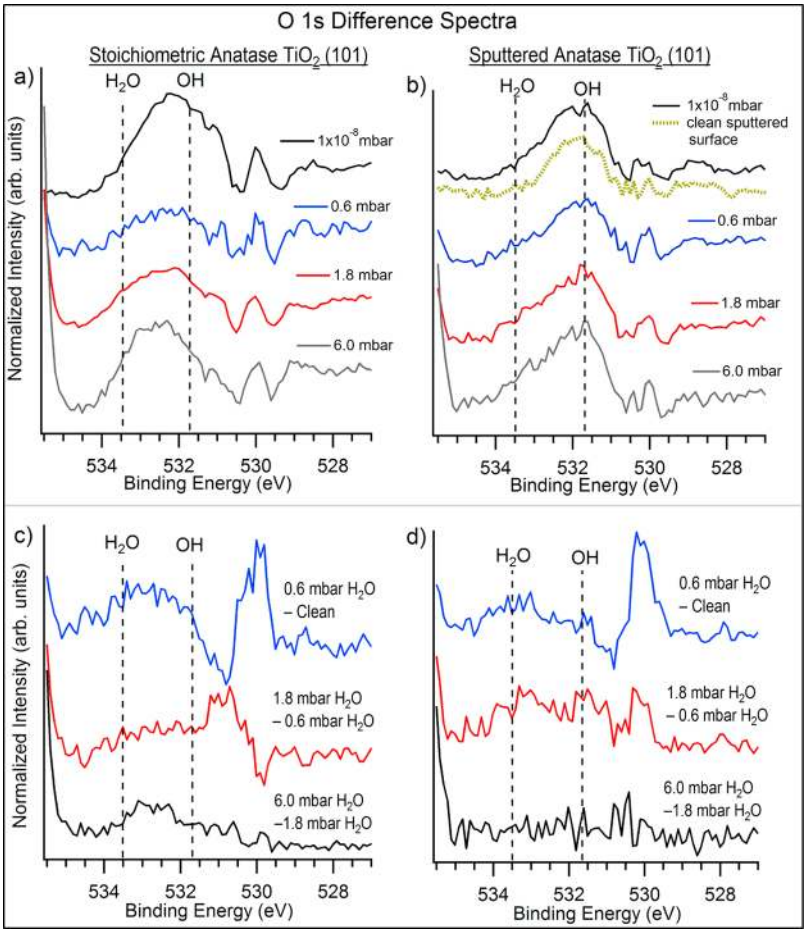

Figure 6. Difference spectra generated from the water dosed surface. (a) and (c) are from stoichiometric anatase TiO_2(101), (b) and (d) are from sputtered anatase TiO_2(101). Details of how the difference spectra are obtained is given in the text.

suggesting they are due to chemisorbed species. Figure 7 shows difference spectra for the two surfaces, obtained by subtracting the clean surface data from the data recorded after water exposure and subsequent evacuation of the near-ambient pressure cell to 1×10^{-8} mbar. The difference spectra look very similar for both surfaces. The peak shape is consistent with the majority of the adsorbed water at this pressure being in the dissociated state, although there does appear to be some asymmetry in the peak, suggesting there may be some remaining molecular water. It must be noted that induced water dissociation by the X-ray beam on the surface cannot fully be ruled out, although no changes in the spectra were observed over time, and water dissociation was not observed by Herman et al. when investigating methanol and water adsorption on the anatase TiO_2(101) surface.[41]

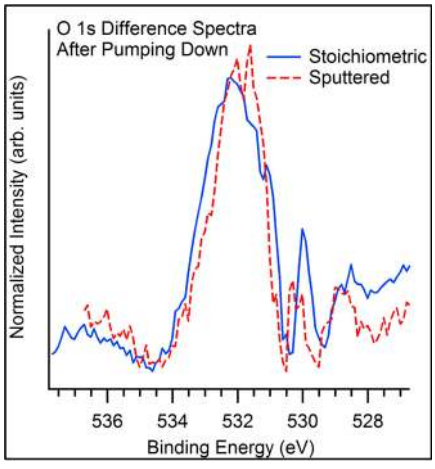

Figure 7. Difference spectra for the stoichiometric and sputtered surfaces. The spectra were obtained by subtracting the clean surface data from the data recorded after water exposure and subsequent evacuation of the near-ambient pressure cell to 1×10^{-8} mbar.

CONCLUSIONS

We have shown that on the anatase TiO_2(101) surface O-vacancies created following argon cluster ion sputtering tend to move subsurface. Cluster Ar^+ ion etching leads to the appearance of Ti^{3+} at or near the surface associated with O-vacancies. In the O 1s spectra we see two new features upon reduction of the surface, which may be related to changes in the local structure. The results with regards to water adsorption at pressures up to 6 mbar indicate that water adsorbs in a mixed dissociative and molecular state at room temperature at pressures of 0.6 mbar and above on both the stoichiometric and sputtered surfaces, and adsorption reaches a saturation point between 0.6 and 1.8 mbar on both surfaces at room temperature. There is little difference in reactivity with regards to water adsorption on both a sputtered and sputtered surface. This supports the suggestions that anatase demonstrates superior photocatalytic activity over rutile due to the tendency

DOI: 10.1021/acs.jpcc.5b02732
J. Phys. Chem. C 2015, 119, 13682−13690

of oxygen vacancies to lie subsurface and therefore are able to contribute to photocatalysis without being quenched by adsorbates.

■ ASSOCIATED CONTENT

Supporting Information

Wide scan of a clean anatase TiO_2(101) surface (S.1); hard X-ray photoelectron O 1s spectra of the anatase TiO_2(101) surface at various depths (S.2); C 1s spectrum of the anatase TiO_2 (101) surface after several hours in high vacuum (S.3). The Supporting Information is available free of charge on the ACS Publications website at DOI: 10.1021/acs.jpcc.5b02732.

■ AUTHOR INFORMATION

Corresponding Author

*E-mail: a.g.thomas@manchester.ac.uk.

Notes

The authors declare no competing financial interest.

■ ACKNOWLEDGMENTS

M.J.J. thanks EPSRC (U.K.) for the award of a studentship through the NowNano Doctoral Training Centre (Grant number EP/G03737X/1). A.G.T. and C.M. thank The University of Manchester for funding.

■ ABBREVIATIONS

NAP-XPS: near-ambient pressure X-ray photoelectron spectroscopy
BE: binding energy
GE: grazing angle
NE: normal angle
GL: Gaussian:Lorentzian

■ REFERENCES

(1) Diebold, U. The Surface Science of Titanium Dioxide. *Surf. Sci. Rep.* **2003**, *48*, 53−229.
(2) Deák, P.; Aradi, B.; Frauenheim, T. Polaronic Effects in TiO_2 Calculated by the HSE06 Hybrid Functional: Dopant Passivation by Carrier Self-Trapping. *Phys. Rev. B* **2011**, *83*, 155207.
(3) Kitano, M.; Takeuchi, M.; Matsuoka, M.; Thomas, J. A.; Anpo, M. Photocatalytic Water Splitting Using Pt-Loaded Visible Light-Responsive TiO_2 Thin Film Photocatalysts. *Catal. Today* **2007**, *120*, 133−138.
(4) Eder, D.; Motta, M.; Windle, A. H. Iron-Doped Pt−TiO_2 Nanotubes for Photocatalytic Water Splitting. *Nanotechnology* **2009**, *20*.
(5) Le, T. T.; Akhtar, M. S.; Park, D. M.; Lee, J. C.; Yang, O. B. Water Splitting on Rhodamine-B Dye Sensitized Co-Doped TiO_2 Catalyst under Visible Light. *Appl. Catal., B* **2012**, *111*, 397−401.
(6) Oregan, B.; Grätzel, M. A Low-Cost, High-Efficiency Solar-Cell Based on Dye-Sensitized Colloidal TiO_2 Films. *Nature* **1991**, *353*, 737−740.
(7) Bakardjieva, S.; Šubrt, J.; Štengl, V.; Dianez, M. J.; Sayagues, M. J. Photoactivity of Anatase−Rutile TiO_2 Nanocrystalline Mixtures Obtained by Heat Treatment of Homogeneously Precipitated Anatase. *Appl. Catal., B* **2005**, *58*, 193−202.
(8) Scanlon, D. O.; Dunnill, C. W.; Buckeridge, J.; Shevlin, S. A.; Logsdail, A. J.; Woodley, S. M.; Catlow, C. R. A.; Powell, M. J.; Palgrave, R. G.; Parkin, I. P.; et al. Band Alignment of Rutile and Anatase TiO_2. *Nat. Mater.* **2013**, *12*, 798−801.
(9) Mu, Q. H.; Li, Y. G.; Wang, H. Z.; Zhang, Q. H. Self-Organized TiO_2 Nanorod Arrays on Glass Substrate for Self-Cleaning Antireflection Coatings. *J. Colloid Interface Sci.* **2012**, *365*, 308−313.
(10) So, S. G.; Lee, K.; Schmuki, P. Ru-Doped TiO_2 Nanotubes: Improved Performance in Dye-Sensitized Solar Cells. *Phys. Status Solidi RRL* **2012**, *6*, 169−171.
(11) Liao, J. Y.; Lin, H. P.; Chen, H. Y.; Kuang, D. B.; Su, C. Y. High-Performance Dye-Sensitized Solar Cells Based on Hierarchical Yolk-Shell Anatase TiO_2 Beads. *J. Mater. Chem.* **2012**, *22*, 1627−1633.
(12) Swierk, J. R.; Mallouk, T. E. Design and Development of Photoanodes for Water-Splitting Dye-Sensitized Photoelectrochemical Cells. *Chem. Soc. Rev.* **2013**, *42*, 2357−2387.
(13) Thomas, A. G.; Flavell, W. R.; Mallick, A. K.; Kumarasinghe, A. R.; Tsoutsou, D.; Khan, N.; Chatwin, C.; Rayner, S.; Smith, G. C.; Stockbauer, R. L.; et al. Comparison of the Electronic Structure of Anatase and Rutile TiO_2 Single-Crystal Surfaces Using Resonant Photoemission and X-ray Absorption Spectroscopy. *Phys. Rev. B* **2007**, *75*.
(14) Setvin, M.; Hao, X.; Daniel, B.; Pavelec, J.; Novotny, Z.; Parkinson, G. S.; Schmid, M.; Kresse, G.; Franchini, C.; Diebold, U. Charge Trapping at the Step Edges of TiO_2 Anatase (101). *Angew. Chem., Int. Ed.* **2014**, *53* (18), 4714−4716.
(15) Wendt, S.; Sprunger, P. T.; Lira, E.; Madsen, G. K. H.; Li, Z. S.; Hansen, J. O.; Matthiesen, J.; Blekinge-Rasmussen, A.; Laegsgaard, E.; Hammer, B.; et al. The Role of Interstitial Sites in the Ti 3d Defect State in the Band Gap of Titania. *Science* **2008**, *320*, 1755−1759.
(16) He, Y. B.; Dulub, O.; Cheng, H. Z.; Selloni, A.; Diebold, U. Evidence for the Predominance of Subsurface Defects on Reduced Anatase TiO_2(101). *Phys. Rev. Lett.* **2009**, *102*, 106105.
(17) Cheng, H. Z.; Selloni, A. Surface and Subsurface Oxygen Vacancies in Anatase TiO_2 and Differences with Rutile. *Phys. Rev. B* **2009**, *79*, 092101.
(18) Setvín, M.; Aschauer, U.; Scheiber, P.; Li, Y.-F. F.; Hou, W.; Schmid, M.; Selloni, A.; Diebold, U.; Setvin, M. Reaction of O_2 with Subsurface Oxygen Vacancies on TiO_2 Anatase (101). *Science* **2013**, *341*, 988−991.
(19) Deák, P.; Aradi, B.; Frauenheim, T. Quantitative Theory of the Oxygen Vacancy and Carrier Self-Trapping in Bulk TiO_2. *Phys. Rev. B* **2012**, *86*, 195206.
(20) Walle, L. E.; Borg, A.; Johansson, E. M. J.; Plogmaker, S.; Rensmo, H.; Uvdal, P.; Sandell, A. Mixed Dissociative and Molecular Water Adsorption on Anatase TiO_2(101). *J. Phys. Chem. C* **2011**, *115*, 9545−9550.
(21) He, Y.; Tilocca, A.; Dulub, O.; Selloni, A.; Diebold, U. Local Ordering and Electronic Signatures of Submonolayer Water on Anatase TiO_2(101). *Nat. Mater.* **2009**, *8*, 585−589.
(22) Herman, G. S.; Dohnálek, Z.; Ruzycki, N.; Diebold, U. Experimental Investigation of the Interaction of Water and Methanol with Anatase−TiO_2(101). *J. Phys. Chem. B* **2003**, *107*, 2788−2795.
(23) Patrick, C. E.; Giustino, F. Structure of a Water Monolayer on the Anatase TiO_2(101). *Phys. Rev. Appl.* **2014**, *2*, 014001.
(24) Newberg, J. T.; Starr, D. E.; Yamamoto, S.; Kaya, S.; Kendelewicz, T.; Mysak, E. R.; Porsgaard, S.; Salmeron, M. B.; Brown, G. E.; Nilsson, A.; et al. Formation of Hydroxyl and Water Layers on MgO Films Studied with Ambient Pressure XPS. *Surf. Sci.* **2011**, *605*, 89−94.
(25) Zhang, X.; Ptasinska, S. Dissociative Adsorption of Water on an H_2O/GaAs(100) Interface: In Situ Near-Ambient Pressure XPS Studies. *J. Phys. Chem. C* **2014**, *118*, 4259−4266.
(26) Haubrich, J.; Quiller, R. G.; Benz, L.; Liu, Z.; Friend, C. M. In Situ Ambient Pressure Studies of the Chemistry of NO_2 and Water on Rutile TiO_2(110). *Langmuir* **2010**, *26*, 2445−2451.
(27) Rosseler, O.; Sleiman, M.; Montesinos, V. N.; Shavorskiy, A.; Keller, V.; Keller, N.; Litter, M. I.; Bluhm, H.; Salmeron, M.; Destaillats, H. Chemistry of NO_x on TiO_2 Surfaces Studied by Ambient Pressure XPS: Products, Effect of UV Irradiation, Water, and Coadsorbed K^+. *J. Phys. Chem. Lett.* **2013**, *4*, 536−541.
(28) Ketteler, G.; Yamamoto, S.; Bluhm, H.; Andersson, K.; Starr, D. E.; Ogletree, D. F.; Ogasawara, H.; Nilsson, A.; Salmeron, M. The Nature of Water Nucleation Sites on TiO_2(110) Surfaces Revealed by Ambient Pressure X-ray Photoelectron Spectroscopy. *J. Phys. Chem. C* **2007**, *111*, 8278−8282.

DOI: 10.1021/acs.jpcc.5b02732
J. Phys. Chem. C 2015, 119, 13682−13690

(29) Jackman, M. J.; Thomas, A. G. Adsorption and Photocatalytic Degradation of 3-Fluoroaniline on Anatase TiO_2(101): A Photoemission and Near-Edge X-ray Absorption Fine Structure Study. *J. Phys. Chem. C* **2014**, *118*, 2028−2036.
(30) Armitage, D. A.; Grant, D. M. Characterisation of Surface-Modified Nickel Titanium Alloys. *Mater. Sci. Eng., A* **2003**, *349*, 89−97.
(31) Lu, G.; Bernasek, S. L.; Schwartz, J. Oxidation of a Polycrystalline Titanium Surface by Oxygen and Water. *Surf. Sci.* **2000**, *458*, 80−90.
(32) Bertoti, I.; Mohai, M.; Sullivan, J. L.; Saied, S. O. Surface Characterization of Plasma-Nitrided Titanium—An XPS Study. *Appl. Surf. Sci.* **1995**, *84*, 357−371.
(33) Kurtz, R. L. UHV-Cleaved Single Crystal $Ti_2O_3(10\bar{1}2)$ by UPS and XPS. *Surf. Sci. Spectra* **1998**, *5*, 182.
(34) Mayer, J. T.; Diebold, U.; Madey, T. E.; Garfunkel, E. Titanium and Reduced Titania Overlayers on Titanium Dioxide (110). *J. Electron Spectrosc. Relat. Phenom.* **1995**, *73*, 1−11.
(35) Syres, K. L.; Thomas, A. G.; Flavell, W. R.; Spencer, B. F.; Bondino, F.; Malvestuto, M.; Preobrajenski, A.; Grätzel, M. Adsorbate-Induced Modification of Surface Electronic Structure: Pyrocatechol Adsorption on the Anatase TiO_2(101) and Rutile TiO_2(110) Surfaces. *J. Phys. Chem. C* **2012**, *116*, 23515−23525.
(36) Perron, H.; Vandenborre, J.; Domain, C.; Drot, R.; Roques, J.; Simoni, E.; Ehrhardt, J.-J.; Catalette, H. Combined Investigation of Water Sorption on TiO_2 Rutile (110) Single Crystal Face: XPS vs Periodic DFT. *Surf. Sci.* **2007**, *601*, 518−527.
(37) Mudd, J. J.; Lee, T.-L.; Muñoz-Sanjosé, V.; Zúñiga-Pérez, J.; Hesp, D.; Kahk, J. M.; Payne, D. J.; Egdell, R. G.; McConville, C. F. Hard X-ray Photoelectron Spectroscopy as a Probe of the Intrinsic Electronic Properties of CdO. *Phys. Rev. B* **2014**, *89*, 035203.
(38) Chambers, S. A.; Droubay, T.; Kaspar, T. C.; Gutowski, M. Experimental Determination of Valence Band Maxima for $SrTiO_3$, TiO_2, and SrO and the Associated Valence Band Offsets with Si(001). *J. Vac. Sci. Technol., B: Microelectron. Nanometer Struct.–Process., Meas., Phenom.* **2004**, *22*, 2205.
(39) Göpel, W.; Anderson, J. .; Frankel, D.; Jaehnig, M.; Phillips, K.; Schäfer, J.; Rocker, G. Surface Defects of TiO_2(110): A Combined XPS, XAES, and ELS Study. *Surf. Sci.* **1984**, *139*, 333−346.
(40) Blomquist, J.; Walle, L. E.; Uvdal, P.; Borg, A.; Sandell, A. Water Dissociation on Single Crystalline Anatase TiO_2(001) Studied by Photoelectron Spectroscopy. *J. Phys. Chem. C* **2008**, *112*, 16616−16621.
(41) Herman, G. S.; Dohnalek, Z.; Ruzycki, N.; Diebold, U. Experimental Investigation of the Interaction of Water and Methanol with Anatase−TiO_2(101). *J. Phys. Chem. B* **2003**, *107*, 2788−2795.
(42) Beatham, N.; Orchard, A. F.; Thornton, G. X-ray and UV Photoelectron Spectra of the Metal Sesquioxides. *J. Phys. Chem. Solids* **1981**, *42*, 1051−1055.
(43) Bundaleski, N.; Silva, A. G.; Schröder, U.; Moutinho, A. M. C.; Teodoro, O. M. N. D. Adsorption Dynamics of Water on the Surface of TiO_2(110). *J. Phys. Conf. Ser.* **2010**, *257*, 012008.
(44) Scheiber, P.; Fidler, M.; Dulub, O.; Schmid, M.; Diebold, U.; Hou, W.; Aschauer, U.; Selloni, A. Subsurface Mobility of Oxygen Vacancies at the TiO_2 Anatase (101) Surface. *Phys. Rev. Lett.* **2012**, *109*, 136103.
(45) Seah, M. P.; Dench, W. A. Quantitative Electron Spectroscopy of Surfaces: A Standard Data Base for Electron Inelastic Mean Free Paths in Solids. *Surf. Interface Anal.* **1979**, *1*, 2−11.
(46) Eriksen, S.; Egdell, R. G. Electronic Excitations at Oxygen Deficient TiO_2(110) Surfaces: A Study by EELS. *Surf. Sci.* **1987**, *180*, 263−278.
(47) Cox, P. A.; Egdell, R. G.; Eriksen, S.; Flavell, W. R. The High-Resolution Electron-Energy-Loss Spectrum of TiO_2(110). *J. Electron Spectrosc. Relat. Phenom.* **1986**, *39*, 117−126.
(48) Pang, C. L.; Lindsay, R.; Thornton, G. Structure of Clean and Adsorbate-Covered Single-Crystal Rutile TiO_2 Surfaces. *Chem. Rev.* **2013**, *113*, 3887−3948.
(49) Li, Y.; Gao, Y. Interplay between Water and TiO_2 Anatase (101) Surface with Subsurface O. *Phys. Rev. Lett.* **2014**, *112*, 206101.
(50) Deák, P.; Kullgren, J.; Frauenheim, T. Polarons and Oxygen Vacancies at the Surface of Anatase TiO_2. *Phys. Status Solidi RRL.* **2014**, *8*, 583−586.
(51) Yamamoto, S.; Bluhm, H.; Andersson, K.; Ketteler, G.; Ogasawara, H.; Salmeron, M.; Nilsson, A. In Situ X-ray Photoelectron Spectroscopy Studies of Water on Metals and Oxides at Ambient Conditions. *J. Phys.: Condens. Matter* **2008**, *20*, 184025.
(52) Ketteler, G.; Yamamoto, S.; Bluhm, H.; Andersson, K.; Starr, D. E. E.; Ogletree, D. F. F.; Ogasawara, H.; Nilsson, A.; Salmeron, M. The Nature of Water Nucleation Sites on TiO_2(110) Surfaces Revealed by Ambient Pressure X-ray Photoelectron Spectroscopy. *J. Phys. Chem. C* **2007**, *111*, 8278−8282.
(53) Gan, S.; Liang, Y.; Baer, D. R.; Sievers, M. R.; Herman, G. S.; Peden, C. H. F. Effect of Platinum Nanocluster Size and Titania Surface Structure upon CO Surface Chemistry on Platinum-Supported TiO_2(110). *J. Phys. Chem. B* **2001**, *105*, 2412−2416.
(54) Suriye, K.; Jongsomjit, B.; Satayaprasert, C.; Praserthdam, P. Surface Defect (Ti^{3+}) Controlling in the First Step on the Anatase TiO_2 Nanocrystal by Using Sol−Gel Technique. *Appl. Surf. Sci.* **2008**, *255*, 2759−2766.
(55) Sorescu, D. C.; Civiš, S.; Jordan, K. D. Mechanism of Oxygen Exchange between CO_2 and TiO_2(101) Anatase. *J. Phys. Chem. C* **2014**, *118*, 1628−1639.

DOI: 10.1021/acs.jpcc.5b02732
J. Phys. Chem. C 2015, 119, 13682−13690